

Available online at www.sciencedirect.com**Energy
Procedia**

Energy Procedia 1 (2009) 1941–1947

www.elsevier.com/locate/procedia

GHGT-9

A numerical study of transport and spreading of gases from natural analogues of gas-seepage through the seafloor

¹Lars Inge Enstad^{a,b}, Guttorm Alendal^c, Peter M. Haugan^b*Bergen Center for Computational Science, UNIFOB, Thormøhlens gt. 55, Bergen N-5008, Norway**^bGeophysical Institute, University of Bergen, Allegaten 70, Bergen N-5007, Norway**^cDepartment of Mathematics, University of Bergen, Johannes Bruns gt. 12, Bergen N-5007, Norway*

Abstract

Natural leakages of CO₂ are reported in the literature at mid ocean ridges and CH₄ seepages in hydrocarbon rich areas. These could potentially serve as natural analogues of leakages from CO₂ storages. In this study we have developed a model tool for the rise and dissolution of droplets or bubbles of these gases and the subsequent spreading of the compounds. The preliminary results shows some of the same trends as has been reported on observations from natural gas leakages. The model has been setup for an idealized natural CO₂ leakage in the deep ocean to illustrate how the model can represent such a leakage.

© 2009 Elsevier Ltd. Open access under [CC BY-NC-ND license](https://creativecommons.org/licenses/by-nc-nd/4.0/).

Keywords: Gas leakage; Bubble Dynamics; CO₂ ; Dissolution

¹ Corresponding author. Tel.: +47-55-584167; fax: +47-55-589883.

E-mail address: lars.inge.enstad@bccs.uib.no.

1. Introduction

A motivation for studying dissolution and spreading of liquid or gaseous CO_2 in the ocean comes from the desire to mitigate anthropogenic CO_2 otherwise emitted to the atmosphere (IPCC [1]). Some of the options suggested are geological storage, storage in the ocean or storage in deep water sediments. CO_2 dissolution and spreading is a determining factor both for ocean storage and to predict the fate of leakages from subsea underground storages. Natural analogues of gas leakages at the seafloor occur at several places around the world (Judd and Hovland [2]). Hydro carbons mostly consisting of CH_4 , are leaked in hydrocarbon rich reach areas where one usually finds oil exploration. In these areas the geological conditions are similar to what one would expect to find near potential CO_2 sequestration sites, but the behavior of CH_4 in seawater is quite distinct from that of CO_2 . Natural leakage of CO_2 on the other hand has been observed at Mid Ocean Ridges (Sakai [3], Lupton [4] and Inagaki [5]) near underwater volcanic areas where gradients of temperature and other dynamically active tracers are high. The geological conditions are also quite different from sites considered for CO_2 storage. CO_2 chemical properties are such that at around 400–500 meters depth it changes from gas form to liquid form, and since it is more compressible than seawater it becomes denser at around 2500 meters. Most of the observed natural leakages of CO_2 are located at 1400 to 1600 meters depth. Released CO_2 will therefore tend to form droplets rising and dissolving in the water column. It should be possible to improve models for dissolution and spreading of CO_2 in seawater by means of comparison to observation of natural sources of CO_2 . The study of natural sources leaked at the seabottom is also interesting from a phenomenological perspective.

Several investigations have been performed to clarify the fate of rising CO_2 droplets in the ocean, using in situ experiments (Brewer [6]), lab experiments (Bigalke [7]) and modelling efforts (Alendal and Drange [8], Chen [9], Gangstø et al. [10]). Comparison between sophisticated models and in situ experiments and measurements has been done by Brewer et al. [11] and McGinnis et al. [12]. Earlier studies have focused on the rise and dissolution of droplets or bubbles. The present study differs from Brewer et al. [11] since a larger domain is employed and exact replication of small scale phenomena is not expected.

In this study the MIT general circulation model (MITgcm, <http://mitgcm.org/>) has been coupled with a single droplet/bubble model. Some modifications have been done to the latter incorporating new parameterizations of solubilities and the drag coefficient. Since, to our knowledge, no measurements of the plume of dissolved CO_2 above natural leakages has been available until recently, the comparison between the model and measurements is limited to CH_4 seepages in the North Sea. Results from an idealized setup for a natural CO_2 seepage is shown to illustrate how the model can represent these phenomena.

2. Method

To be able to simulate both the rise and dissolution of droplets/bubbles and the subsequent spreading of the dissolved compounds, the MITgcm has been coupled to a single droplet/bubble model. The latter has previously been used in a study of the rise of single CO_2 droplets by Gangstø et al. [9]. The MITgcm can be used on a wide range of scales from global climate studies to small scale channel flows. It also has a non-hydrostatic capability which is important when transferring momentum from the single droplet/bubble model to the surrounding water. The single droplet/bubble model integrates position, mass and size of the droplet/bubbles (particles hereafter). The governing equations are the mass transfer

$$\frac{dm}{dt} = -Sh d_e \pi D_v (C - C_s) \quad (1)$$

Sh is the Sherwood number given by the correlation, d_e is the equivalent diameter, D_v is the diffusion C is the solubility and C_s is the ambient concentration. The momentum equations are given as a balance between the buoyancy force and the drag force exerted on the particles. The rise velocity is then given as

$$U = \left(\frac{8 g r_e (\rho - \rho_p)}{3 C_d \rho} \right)^{0.5} \quad (2)$$

Here g is the gravitational acceleration, r_e is the equivalent radius, ρ is the density of the surrounding water, ρ_p is the density of the particle and C_d is the drag coefficient. The position of a particle is stepped forward in time using a fifth order Runge Kutta method. Important parameters to be estimated in these equations are the solubility C in the mass transfer equation, and the drag coefficient C_d in the rise velocity equation. A new implementation for the solubilities has been used based on Teng et al. [13] for solubility of clean CO_2 droplets and Chen [8] for hydrate coated CO_2 droplets and Duan and Mao [14] for CH_4 bubbles. Figure (1a) shows comparison between time development of the equivalent radius in the model with existing measurements of hydrate coated CO_2 droplet dissolution (Brewer et al. [5]). In the same way Figure (1b) represents same type of plot but for the time development of equivalent radius of a clean bubble compared with an empirical correlation by Rehder et al. [15]. Both figures show favorable comparison between the model and the in situ measurements.

The drag coefficient previously used by Gangstø et al. [9] was the parameterization derived by Bozanna and Dente [16]. This was a drag parameterization originally developed for gas bubbles near atmospheric pressure, and has been shown to disagree with recently published experimental data (Bigalke [7]). A different drag parameterization than what was used by Gangstø et al. [9] has been incorporated to improve the calculation of the rise velocity (Bigalke [17]). The drag parameterization has been developed for clean and hydrate covered CO_2 droplets and will be published elsewhere, but has shown good comparison with experimental data.

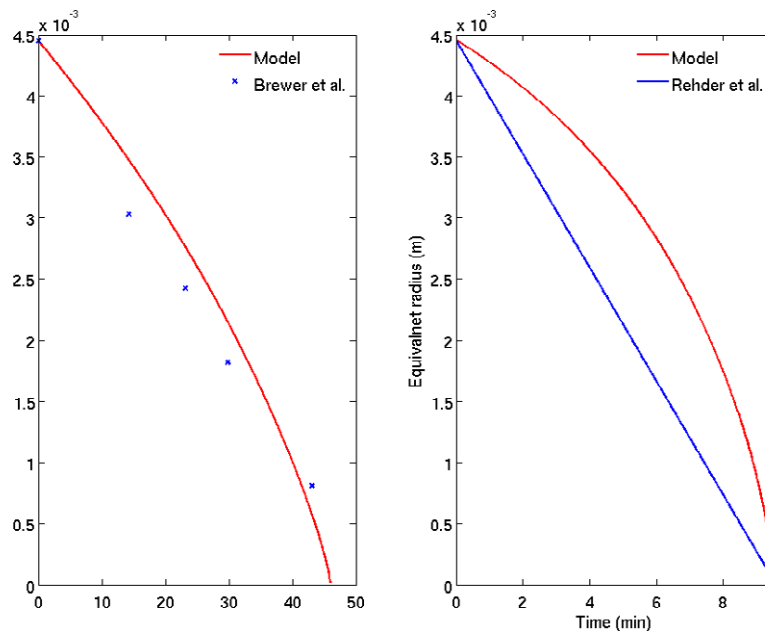


Figure 1. Time development of equivalent radius of CO_2 droplets and CH_4 bubbles. The model results are compared to ocean experiments.

From the single particle model we obtain the mass deposited at each position of the particle. This mass is transferred to the general circulation model. During this process the distribution of the dissolved mass is interpolated to the MITgcm model grid. The vertical distribution of the dissolved mass in MITgcm is verified by comparing it with the distributed mass from a run with the single particle model alone. Also the momentum transfer from the single particle model is added in the momentum equation in MITgcm. This is possible because of the non-hydrostatic possibility in MITgcm. The drag force is given by

$$F_d = 1/2 \rho C_d A |(U - U_s)|(U - U_s) \quad (3)$$

where A is the projected area U_s is the vertical velocity component of the surrounding fluid.

To keep track of the particles from they are released at the bottom to they are completely dissolved or reach the surface, an interface routine between MITgcm and the single particle model is developed. In this routine the data of the particles are stored in a dynamical pointer structure. Advection of each particle is computed based on the velocity field in MITgcm. The boundary conditions are given as periodic in the horizontal directions and a no-slip condition at the bottom and free slip at the surface. Particles moving out of the domain are deleted.

3. Results

3.1. CH₄ seepage

To compare the ability of the coupled model to represent the vertical distribution of dissolved mass, a qualitative comparison with in situ data presented in Leifer and Judd [18] was performed. They presented averages of bottle cast measurements giving vertical profiles of CH₄ concentrations above and beside pockmark areas in the North Sea. The results show a peak in the concentration at some distance from the bottom. They explain this peak by presenting the “bubble deposition hypothesis” which implies that upwelling flow creates the maximum concentration at a vertical distance from the source. By running the model both with and without the transfer of vertical momentum it should be possible to give an indication of the validity of this transfer in the model.

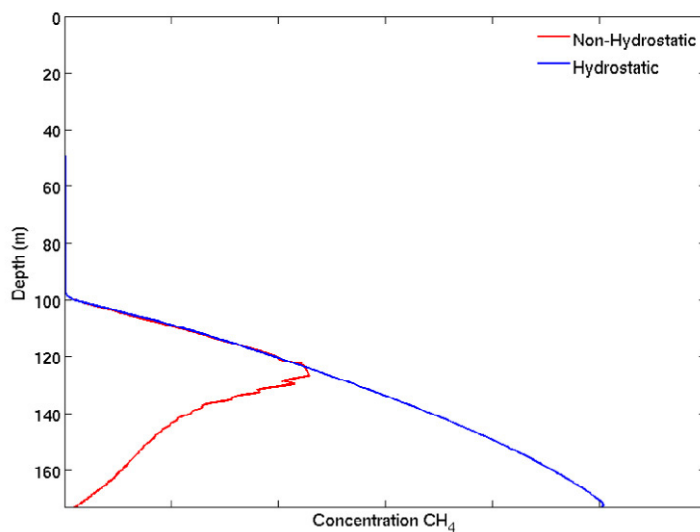


Figure 2. CH₄ concentrations as a function of depth modelled both with and without transfer of momentum from the single particle model.

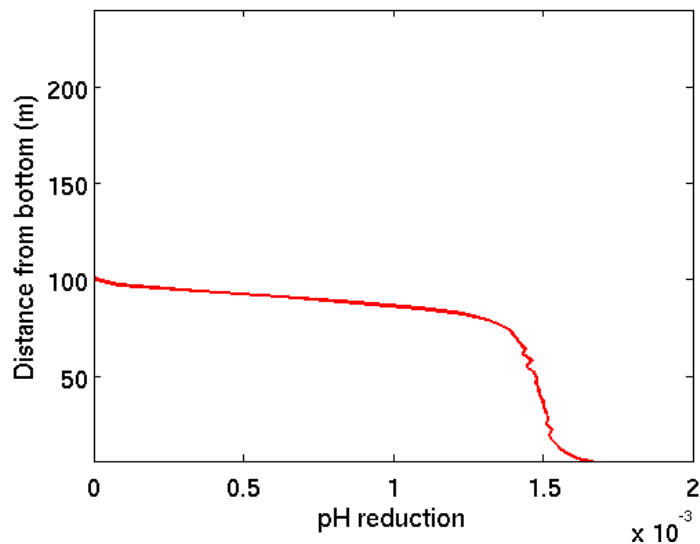
The model setup is simple with a $20 \times 20 \times 350$ grid size and $10 \times 10 \times 175$ meters domain size. The flux at the bottom is given as one bubble each 6 seconds (Hovland and Judd [19]) with a equivalent radius of 4.5 mm. A temperature gradient is introduced giving a stable stratification near the surface. Since most parameters which will determine the bubble deposition depth are unknown and due to the simple setup of the model, only qualitative similarities can be expected.

Figure (2) displays the concentration profile of CH_4 as a function of the depth, both with and without transfer of vertical momentum. Leifer and Judd [16] found a maximum concentration at 100–125 meters depth. With the setup employed in the current numerical experiment we obtain such a maximum at 120 meters depth. In the case where the vertical momentum forcing from the bubbles on the water column is left out, the profile is decreasing away from the bottom. The model results suggest that upwelling flow affects the concentration giving higher concentrations away from the bottom, and that the transfer of vertical momentum is included in a realistic manner.

3.2 CO_2 leakage

The model has been setup for an idealized CO_2 leakage in the deep ocean at 1600 meters depth. The flux used is one droplet of 4.5 mm equivalent diameter released each 6 seconds. The release is distributed over an area of 10×10 meters. Tidal forcing is enforced giving a velocity ellipsoid. The effect of tidal flow on bottom currents was measured by Barry et al. [20]. The diffusivity is set to 5.0×10^{-1} in the horizontal direction and 1.0×10^{-2} in the vertical direction. The domain is $300 \times 300 \times 400$ meters with a grid resolution of $99 \times 99 \times 80$.

Figure (3) shows the pH reduction profile as a function of distance from the bottom above the leakage. The profile shows a linear trend away from the bottom. The larger concentration near the seafloor could be due to the lower velocities close to the bottom and subsequently lower transport.



pH reduction profile above the leakage point as a function of distance from the bottom.

Figure (3) shows the pH reduction profile as a function of distance from the bottom above the leakage. The profile shows a linear trend away from the bottom. The larger concentration near the seafloor could be due to the lower velocities close to the bottom and subsequently lower transport.

In Figure (4) an isosurface of pH reduction of 10^{-4} is shown together with a contour slice of the pH reduction. The higher pH reductions is limited to a narrow band. This corresponds with the measurement of Barry et al. [20], where they measured the pH reduction in the vicinity of liquid CO_2 released beneath the density inversion. For the droplet flux rate used in the present model the pH reduction remains low. In an area with CO_2 seepage there will also be CO_2 slowly diffusing out of the bottom sediment. This will create a larger pH reduction than if CO_2 is only released as droplets. This effect is not included here, but should be added to the model in future studies.

4. Conclusions/Summary

A model has been developed where modeling of rise and dissolution of droplets and bubbles has been combined with the subsequent spreading and transport of the dissolved tracers. The parameterization of the mass transfer and drag coefficient has been verified using experiment and in situ data. Using a simple setup for a pockmark like seepage the model reproduces roughly some of the features found in measurements presented in the literature. The model was also setup in an idealized manner for a CO_2 leakage to illustrate how the model can represent such a leakage.

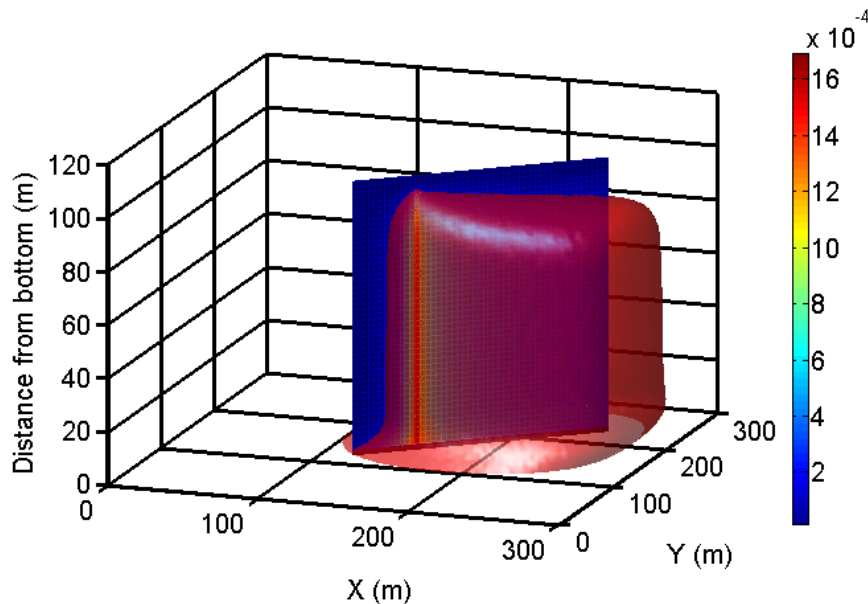


Figure 4. Isosurface of seawater with a pH reduction of 0.0001 together with a slice of contours of the pH reduction

Acknowledgement

This work has been supported by StatoilHydro and Norwegian Academy of Science and Letters through VISTA (6152)

References

1. B. Metz and O. Davidson and H. C. de Coninck and M. Loos and L. A. Meyer(Eds.)] IPCC. Special Report on Carbon Dioxide Capture and Storage. Prepared by Working Group III of the Intergovernmental Panel on Climate Change. Cambridge, United Kingdom and New York, NY, USA, December 2005
2. A. G. Judd and M. Hovland, Seabed fluid flow, Cambridge University Press, New York, 2007
3. H. Sakai, T. Gamo, E-S. Kim et al., Submarine venting of liquid carbon dioxide on a Mariana Arc volcano, *Science*, 248(4959), 1093-1086, 2006
4. J. Lupton et al. Submarine venting of liquid carbon dioxide on a Mariana Arc volcano, *Geochem, Geophys. Geosyst.* 7, (2006)
5. F. Inagaki, M. M. M. Kuypers, U. Tsunogaim et al., Microbial community in a sediment-hosted CO₂ lake of the southern Okinawa Trough hydrothermal system, *PNAS*, 103, 14164-14169, 2006
6. P. G. Brewer, E. T. Peltzer, G. Friederich and G. Rehder, Experimental determination of the fate of rising CO₂ droplets in seawater, *Environ. Sci. Technol.*, 36, 5441-5446, 2002
7. N. K. Bigalke, G. Rehder and G. Gust, Experimental investigation of the rising behavior of CO₂ droplets in seawater under hydrate-forming conditions, *Environ. Sci. Tech.*, 42, 5241-5246, 2008
8. G. Alendal, H. Drange, Two-phase, near field modelling of purposefully released CO₂ in the ocean, *J. Geophys. Res.*, 106, 1085-1096, 2001
9. B. Chen, Y. Song, M. Nishio and M. Akai, Large-eddy simulation of double-plume formation induced by CO₂ dissolution in the ocean, *Tellus, Ser B.*, 55, 723-730, 2003
10. R. Gangstø, P. M. Haugan and G. Alendal, Parameterization of drag and dissolution of rising CO₂ drops in seawater. *Geophys Res Letters*, 32 L10612, 2005
11. P. G. Brewer, B. Chen, R. Warzinski et al., Three-dimensional acoustic monitoring and modeling of a deep-sea CO₂ droplet cloud, *Geophys. Res. Letters*, 33, 2007
12. D. F. McGinnis, J. Greinert, Y. Artemov, S. E. Beaubien and A. Wuest, Fate of rising methane bubbles in stratified waters: How much methane reaches the atmosphere?, *J. Geophys. Res.* 111, C09007, 2006
13. H. Teng, S. M. Masutani, C. M. Kinoshita et al., Solubility of CO₂ in the ocean and its effect on CO₂ dissolution, *Energy Convers. Manag.*, 37, 1029-1038, 1996
14. ZH. Duan and S. Mao, An improved model for calculating methane solubility, density and gas phase composition of methane-bearing aqueous fluids from 273 to 523 K and from 1 to 200 bar. *Geochim. Cosmochim. Acta*, 70, 3369-3386, 2006
15. G. Rehder, P. G. Brewer, E. T. Peltzer and G. Friederich, Enhanced lifetime of methane bubble streams within the deep ocean, *Geophys. Res. Letters*, 29, 2002
16. G. Bozanno and M. Dente, Shape and terminal velocity of single bubble motion: A novel approach, *Comput. Chem. Eng.* 25, 571-576, 2001
17. N. Bigalke, Constraining Hydrate-Mediate transfer of the greenhouse gases CO₂ and CH₄ to the ocean at controlled thermodynamic and hydrodynamic forcing, PhD thesis, 114 pp., In press
18. M. Hovland and A. G. Judd, Seabed Pockmarks and Seepages, Graham & Trotman, 1988
19. I. Leifer and A. G. Judd, Oceanic methane layers: the hydrocarbon seep bubble deposition hypothesis, *Terra Nova*, 2002
20. J. P. Barry, K. R. Buck, C. F. Lovera et al., Effects of direct ocean CO₂ injection on deep-sea meiofauna, *J. Oceanogr.*, 60, 259-766, 2004